

Article

Microgravity-Induced Cell-to-Cell Junctional Contacts Are Counteracted by Antioxidant Compounds in TCam-2 Seminoma Cells

Angela Catizone ^{1,†}, Caterina Morabito ^{2,†}, Marcella Cammarota ³, Chiara Schiraldi ³,
Katia Corano Scheri ¹, Francesca Ferranti ⁴, Maria A. Mariggìò ^{2,*,‡} and Giulia Ricci ^{3,*,‡}

¹ Department of Anatomy, Histology, Forensic-Medicine and Orthopedics, Section of Histology and Embryology, “Sapienza” University of Rome, 00161 Rome, Italy; angela.catizone@uniroma1.it (A.C.); katia.coranoscheri@uniroma1.com (K.C.S.)

² Department of Neuroscience, Imaging and Clinical Sciences and Center for Advanced Studies and Technology (CAST), “G. d’Annunzio” University of Chieti-Pescara, 66100 Chieti, Italy; cmorabit@unich.it

³ Department of Experimental Medicine, Università degli Studi della Campania “Luigi Vanvitelli”, 80138 Naples, Italy; marcella.cammarota@unicampania.it (M.C.); chiara.schiraldi@unicampania.it (C.S.)

⁴ Italian Space Agency (ASI), 00133 Rome, Italy; francesca.ferranti@asi.it

* Correspondence: mariggio@unich.it (M.A.M.); giulia.ricci@unicampania.it (G.R.)

† Equal contribution as first authors.

‡ Equal contribution as senior authors.

Received: 28 October 2020; Accepted: 20 November 2020; Published: 23 November 2020



Abstract: The direct impact of microgravity exposure on male germ cells, as well as on their malignant counterparts, has not been largely studied. In previous works, we reported our findings on a cell line derived from a human seminoma lesion (TCam-2 cell line) showing that acute exposure to simulated microgravity altered microtubule orientation, induced autophagy, and modified cell metabolism stimulating ROS production. Moreover, we demonstrated that the antioxidant administration prevented both TCam-2 microgravity-induced microtubule disorientation and autophagy induction. Herein, expanding previous investigations, we report that simulated microgravity exposure for 24 h induced the appearance, at an ultrastructural level, of cell-to-cell junctional contacts that were not detectable in cells grown at 1 g. In line with this result, pan-cadherin immunofluorescence analyzed by confocal microscopy, revealed the clustering of this marker at the plasma membrane level on microgravity exposed TCam-2 cells. The upregulation of cadherin was confirmed by Western blot analyses. Furthermore, we demonstrated that the microgravity-induced ROS increase was responsible for the distribution of cadherin nearby the plasma membrane, together with beta-catenin since the administration of antioxidants prevented this microgravity-dependent phenomenon. These results shed new light on the microgravity-induced modifications of the cell adhesive behavior and highlight the role of ROS as microgravity activated signal molecules.

Keywords: TCam-2 seminoma cells; microgravity; antioxidant compounds; cell adhesion; mitohormesis

1. Introduction

Nowadays, space exploration is a challenge that makes it necessary to deal with the hostile environment outside the Earth. This stimulated the birth of a novel field of scientific research called “Space biology”. A consistent part of this area of research has addressed the study of the role of gravitational forces in biological processes, studying the effects of weightlessness, real or simulated, on living systems. In this way, “Space biology” insights allowed us to obtain an impressive mass

of knowledge revealing the tight interplay among mechanical forces, cell metabolism, and cell behavior [1–4], as well as to put a spotlight on the importance of physical forces on cell physiology. To this concern, microgravity-related cell modifications have been studied generating an increasing body of evidence, which indicates how different aspects of cell physiology are tightly connected with the gravitational force [5–10]. Indeed, several studies indicated that mammalian cells are able to perceive gravitational force, even if not “mechano-sensitive cells”, and respond to the changes of gravitational force [11–14]. Among them, male germ cells have been revealed to be sensitive to changes of gravitational force [15–21]. Our group focused the attention on TCam-2 cells, derived from a seminoma lesion, that through their malignant transformation, maintain at least partially the phenotypic and molecular features of their normal counterpart [22–24]. For this reason, this represents the best in vitro model to study testicular mitotically active male germ cells. In previous papers, we reported that microgravity transiently modified structural features of TCam-2 cells, such as cell shape, microtubule organization, and mitochondria morphology, and that these changes came together with the modification of some crucial cell activities. Indeed, we reported that simulated microgravity impaired the TCam-2 cell proliferation rate, promoted autophagy, modified some metabolic parameters, and stimulated reactive oxygen species (ROS) production [25,26].

Notably, we also demonstrated that the microgravity-dependent ROS increase is essential to trigger microgravity-induced TCam-2 cell autophagy and microtubule disorientation, since the administration of antioxidants counteracted these microgravity-dependent cellular responses [26]. In light of these results, the observed ROS production by TCam-2 cells after simulated microgravity exposure is used as molecular signals that allow cells to react to microenvironmental stress.

In the present paper, expanding the already mentioned studies, we evaluated the effect of short-term exposure to simulated microgravity on TCam-2 cell junctional features at the ultrastructural and molecular level. We evaluated beta1 integrin as a marker of the cell to substrate interaction, whereas cadherin and beta-catenin have been studied as markers of the cell-to-cell junctional capability, and possible modulators of cell malignant behavior [27,28]. Moreover, we investigated the effects of antioxidants on these cellular activities, trying to elucidate the role of microgravity-induced ROS production in this peculiar aspect of TCam-2 cell physiology.

2. Materials and Methods

2.1. Equipment and Cell Exposure Parameters

Microgravity conditions were simulated using a desktop random positioning machine (RPM) connected to a control console through standard electrical cables (Dutch Space, Leiden, The Netherlands). This apparatus is a 3D clinostat consisting of two independently rotating frames. One frame is positioned inside the other, exerting a complex net change in orientation on a biological sample mounted in the middle. The degree of microgravity simulation depends on the angular speed and the inclination of the disk. This apparatus does not actually eliminate gravity, but the RPM is a micro-weight simulator based on the principle of “gravity-vector averaging”: It allows a 1 g stimulus to be applied omnidirectionally rather than unidirectionally, and the sum of the gravitational force vectors tends to equal zero. The effects generated by the RPM are comparable to the effects of real microgravity, provided that the direction changes are faster than the response time of the system to the gravity field. The RPM was positioned within an incubator (to maintain the 37 °C temperature and CO₂ and humidity levels).

2.2. Cell Cultures

The human TCam-2 cell line (kindly provided by Prof. Claudio Sette, Rome, Italy) was cultured in a growth medium (RPMI 1640 supplemented with 10% foetal bovine serum and penicillin/streptomycin) at a density of 30×10^3 cells/cm². Twenty-four hours after the cells were seeded, experiments were performed on cells cultured for 24 h at 1 g (CTR) in the same incubator containing the

RPM or at simulated microgravity in the RPM. Where indicated, cells were grown at 1 g or on RPM in the presence of antioxidant compounds, which are: N-acetyl-cysteine (NAC; 1 mM), and 6-hydroxy-2,5,7,8-tetramethylchroman-2-carboxylic acid (Trolox; 100 μ M). The latter compound was solubilized in dimethyl sulfoxide (DMSO) at a concentration of 100 mM and then diluted in a cell medium at a final concentration of 100 μ M. For Western blot analyses and transmission electron microscopy (TEM) analyses, cells were plated in 35 mm Petri dishes. For immunofluorescence staining, cells were plated on glass slides or IBIDI microscopy chambers (IBIDI GmbH, Martinsried, Germany). For SEM analyses, cells were seeded on a round glass coverslip, which were silicone-fixed to the culture dishes at least 48 h before plating. All cell culture holders (microplates, dishes, etc.) were completely filled with the culture medium and placed in both 1 g (CTR) and RPM culture conditions to avoid air bubbles and to minimize the liquid flow. Therefore, the effects of both buoyancy and shear stress during rotation were negligible.

2.3. Electron Microscopy

Cells cultured for electron microscopy purposes were fixed in Glutaraldehyde 2.5% in a cacodylate buffer 0.1 M pH 7.3 ON at 4 °C.

2.3.1. Scanning Electron Microscopy (SEM) Analysis

Glutaraldehyde-fixed cells were rinsed with a cacodylate buffer and then dehydrated with an increasing ethanol percentage (30–90% in water for 5 min, twice 100% for 15 min), treated in a Critical Point Dryer (EMITECH K850), sputter coated with platinum-palladium (Denton Vacuum DESKV), and observed with Supra 40 FESEM (Zeiss).

2.3.2. Transmission Electron Microscopy (TEM) Analysis

Glutaraldehyde-fixed cells were rinsed with a cacodylate buffer for at least 1 h. Then, cells were post-fixed with 1% OsO₄ in a 0.1 M cacodylate buffer, mechanically and gently detached, centrifuged, dehydrated in ethanol, and embedded in epoxy resin. Ultrathin sections (60 nm) were treated with tannic acid and then contrasted with lead hydroxide. Images were acquired using a Libra 120 transmission electron microscope (Zeiss) equipped with a wide-angle dual speed CCD-camera sharp:eye 2 K (4Mpx) operated by the iTEM software (Soft Image System, Münster, Germany).

2.4. Confocal Microscopy Analyses

2.4.1. Immunofluorescence

Cells cultured into IBIDI microscopy chambers were fixed with 4% paraformaldehyde in phosphate buffered saline (PBS) for 10 min at 4 °C and permeabilized with 1% bovine serum albumin and 0.1% Triton X-100 in PBS for 1 h at room temperature. Cells were incubated with the following primary antibodies diluted in PBS containing 1% BSA/0.1% Triton X-100 overnight at 4 °C: Mouse monoclonal anti vimentin (clone V9 cod. MA5-11883, Thermo Fisher Scientific; 1:75 dilution), mouse monoclonal anti pan-cadherin (clone CH-19 cod. MA1-91128, Thermo Fisher Scientific; 1:50 dilution), rabbit polyclonal anti beta1 integrin (clone M106 cod. sc-8978, Santa Cruz Biotechnology, Heidelberg, Germany; 1:50 dilution), mouse monoclonal anti beta-catenin (clone E5 cod. sc-7963, Santa Cruz Biotechnology; 1:50 dilution). After rinsing, samples were incubated with a specific secondary antibody diluted in PBS for 90 min at room temperature (FITC-conjugated donkey anti-rabbit or anti-mouse IgGs or TRITC-conjugated donkey anti-mouse IgGs, Jackson ImmunoResearch, Newmarket Suffolk, UK; 1:200 dilution). Then, samples were washed and mounted in buffered glycerol (0.1 M, pH 9.5).

2.4.2. F-Actin Staining

Cells were fixed with 4% paraformaldehyde in PBS for 10 min at 4 °C, and permeabilized with cold ethanol:acetone (1:1) for 10 min at 4 °C to label F-Actin. After rinsing, cells were incubated with

rhodamine-conjugated phalloidin (1:40 dilution, Invitrogen Molecular Probes, Eugene, OR, USA) for 25 min, washed in PBS, and mounted. Images of each sample were acquired using a Zeiss fluorescence microscope (Axioscope) and a Leica confocal microscope (Laser Scanning TCS SP2) equipped with Kr/Ar and He/Ne lasers.

2.5. Western Blotting

Cells were scraped, lysed, and collected in a sample buffer (62.5 mM Tris-HCl, pH 6.8, 2% SDS, 10% glycerol, 0.1 M dithiothreitol, and 0.002% bromophenol blue). Protein concentrations were determined using a protein assay kit (Bio-Rad DC; Bio-Rad, Segrate, Italy). Cell extracts were separated on 7.5% or 10% (w/v) homogeneous slab gels (40 µg of protein/lane) using SDS-PAGE and then transferred to nitrocellulose membranes (Protran; Whatman-GE Healthcare, Milan, Italy). Membranes were previously hybridized with the following primary antibodies: A mouse monoclonal anti pan-cadherin (1:500 dilution, clone CH-19 cod. MA1-91128, Thermo Fisher Scientific, Monza, Italy), or a rabbit polyclonal anti beta1 integrin (1:500 dilution, clone M106 cod. sc-8978, Santa Cruz Biotechnology), or a mouse monoclonal anti vimentin (1:500 dilution, clone V9 cod. MA5-11883, Thermo Fisher Scientific), and then incubated with horseradish-peroxidase-conjugated anti-mouse or anti-rabbit IgGs (1:10,000 dilution, cod. NA931 or cod. NA934, respectively, GE Healthcare, Cologno Monzese, Italy). The relevant proteins were detected using chemiluminescence kits (Pierce EuroClone SpA, Pero, Italy), and the signals were acquired and analyzed using an image acquisition system (Uvitec mod Alliance 9.7, Uvitec, Cambridge, UK). A mouse monoclonal anti-GAPDH antibody (1:10,000 dilution, Merck SpA, Vimodrone, Italy) was used as a loading control.

2.6. Statistical Analyses

Experimental values are expressed as means ± SEM. Statistical significance was assessed using Student's t-tests with the Prism5 software (GraphPad, San Diego, CA, USA). P-values < 0.05 were considered statistically significant.

2.7. Data Availability Statement

The authors confirm that all data supporting the findings are available without restriction.

3. Results

3.1. Simulated Microgravity Influences the TCam-2 Cell Membrane Surface at Cell-to-Cell Contacts

As previously described, the 24 h exposure to simulated microgravity caused significant TCam-2 cell membrane modifications since the mechano-sensing microvilli-like structures, present on the surface of the cell membrane, collapsed when cultured in the random positioning machine (RPM) [25]. Herein, we focus on the effects induced by simulated microgravity on the surface membrane at the cell-to-cell contacts. In Figure 1, we report representative images of SEM analyses on sub-confluent (A,B,C,D) or confluent (E,F,G,H) cells cultured at 1 g (CTR) or under simulated microgravity (RPM). SEM images showed that sub-confluent cells began to contact each other forming mainly larger sites of interaction when cultured in the RPM condition (Figure 1C,D). This occurs if compared with cells cultured at 1 g, in which the cell-to-cell contacts were characterized by membrane protrusions that are much more thin and similar to filopodia (Figure 1A,B). Even in confluent cells, which appeared as an epithelial-like sheet, the RPM condition caused an evident modification of the cell-to-cell contact area (Figure 1G) that appeared, at high magnification, to be formed by complex membrane interdigitations (Figure 1H), whereas in cells cultured at 1 g the cell-to-cell interface appeared mostly linear (Figure 1E,F).

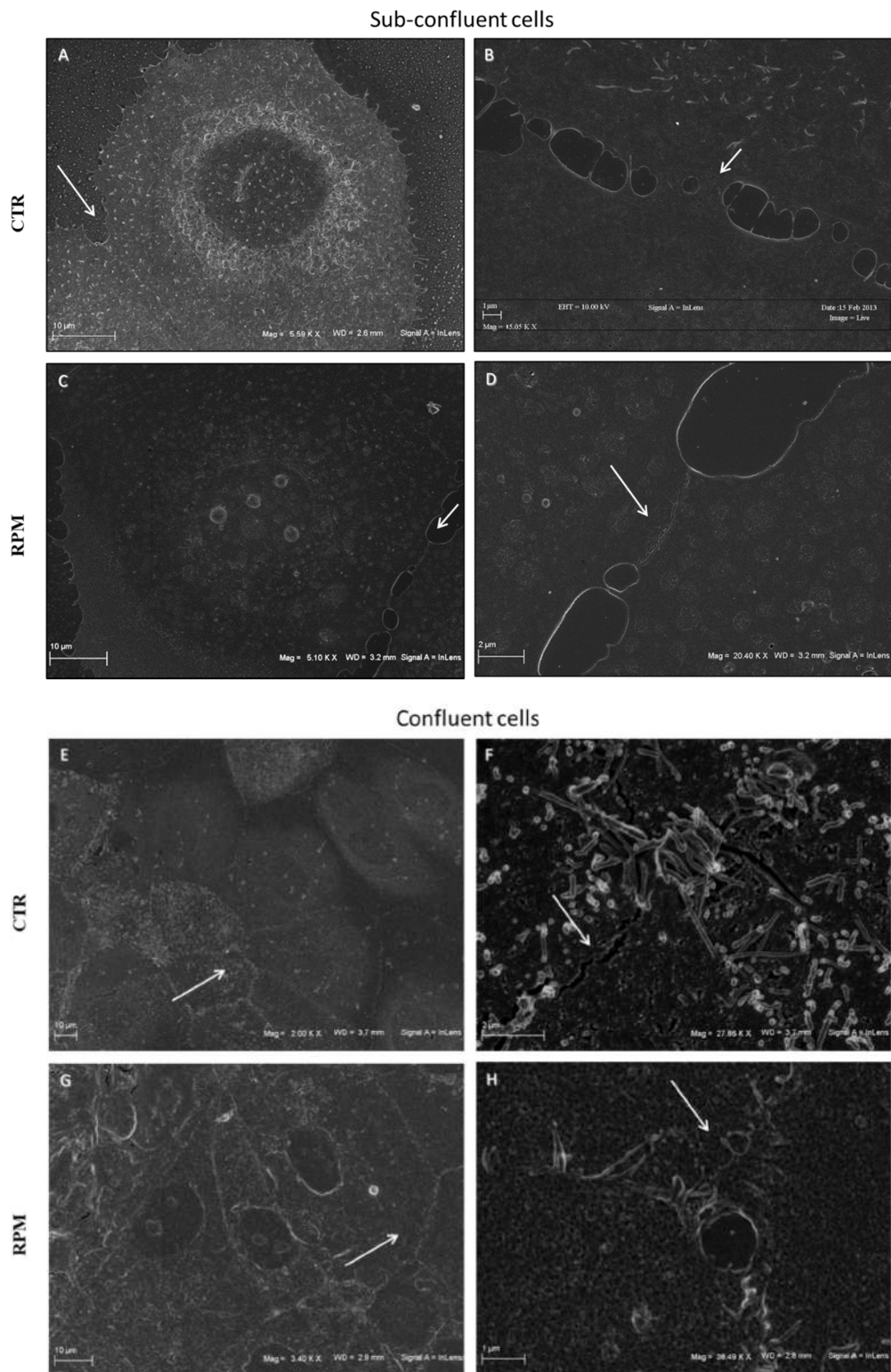


Figure 1. Scanning electron microscopy analyses of TCam-2 seminoma cells exposed for 24 h to 1 g (CTR: **A,B,E,F**) and simulated microgravity (RPM: **C,D,G,H**). In (**A–D**), the images were captured at the periphery of the culture dish where cells are sub-confluent. In (**E–H**), the images were captured in the middle part of the dish where cells are confluent. The arrows in all the figures indicate the regions of plasma membrane, in which cells interact with each other. In (**A,C,E,G**), lower magnifications (from 2000 to 5500 \times) and in (**B,D,F,H**) higher magnifications (from 15,000 to 38,500 \times) are shown.

3.2. Simulated Microgravity Influences the TCam-2 Cell Ultrastructure at the Junctional Level

As already mentioned, TCam-2 seminoma cells grow *in vitro* as an epithelial-like sheet. However, it has been demonstrated that these cells are not able to form ultra-structurally defined adherent junctions when cultured in basal conditions [24,29]. This cellular behavior is common in epithelial transformed cells which partially lose their epithelial features [30,31]. In a previous paper, we described that microgravity exposure induced transient ultrastructural changes such as mitochondria morphological alterations [26] and activation of autophagy [25]. In the present study, the collected images revealed that, after 24 h-exposure to simulated microgravity, the cells showed the formation of adherent junctions (Figure 2C,D), which are not detectable in cells cultured at 1 g (Figure 2A,B). It is evident that in 1 g basal conditions, the membranes of neighboring cells became very close but failed to form electron-dense regions or plaques typical of junctional contacts (Figure 2A,B). In RPM cultured cells, the cell-to-cell interface was very jagged and often engaged in desmosome-like (Figure 2C), as well as by adherent junctions (Figure 2D).

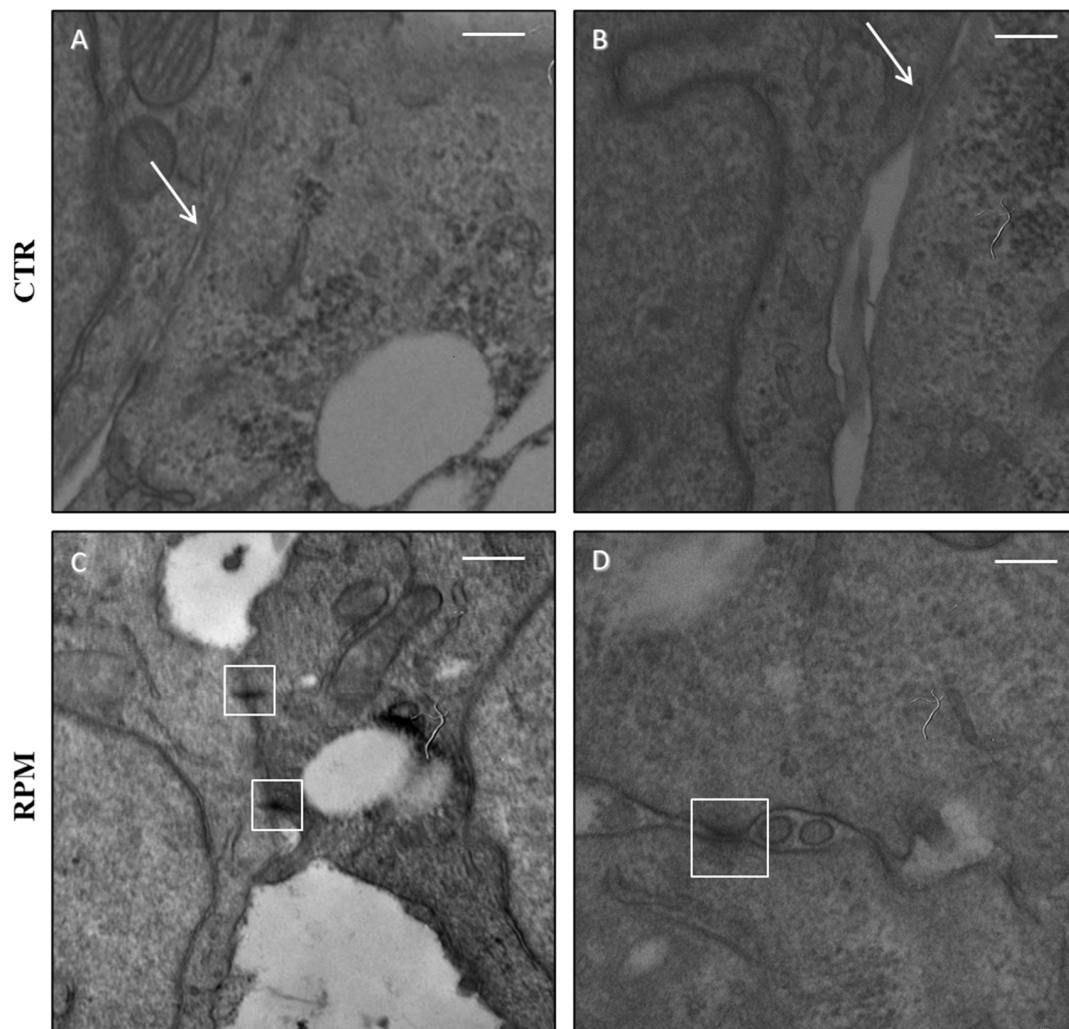


Figure 2. Transmission electron microscopy analyses of cell-to-cell contacts of TCam-2 seminoma cells exposed for 24 h to 1 g (CTR: A,B) and simulated microgravity (RPM: C,D). The arrows in (A,B) indicate the region of plasma membrane in which two cells interact with each other without forming junctions. The white squares in (C,D) indicate desmosome-like and adherent junctions, respectively (BAR: 0.3 μ m).

3.3. Simulated-Microgravity Exposure Modifies the TCam-2 Distribution Pattern of Cadherins but Does Not Influence Beta1 Integrin and Vimentin Localization

The RPM-induced modulation of the ultrastructure of cell-to-cell contacts, observed by electron microscopy, strongly indicated that this experimental condition could modify the distribution pattern and/or the expression levels of adhesion molecules such as cadherins and integrins. We used a pan-cadherin antibody to evaluate the distribution pattern of this class of cell-to-cell adhesion molecules in TCam-2 seminoma cells. As far as integrin is concerned, we focused our attention on the beta1 integrin subunit, since it has been demonstrated that this protein is expressed by TCam-2 seminoma cells [29]. The confocal analyses of cadherin's distribution pattern showed that after RPM exposure (Figure 3B) the cells showed the presence of cadherin at the plasma membrane level with respect to cells cultured at 1 g in which, as expected, the cadherin presence close to the plasma membrane is very limited (Figure 3A). Intriguingly, the co-localization analysis of cadherin and F-Actin in RPM cultured TCam-2 seminoma cells revealed that the localization of these molecules largely overlaps, confirming the presence of stable junctional contacts, which are tightly joined to the actin cytoskeleton (Figure 4).

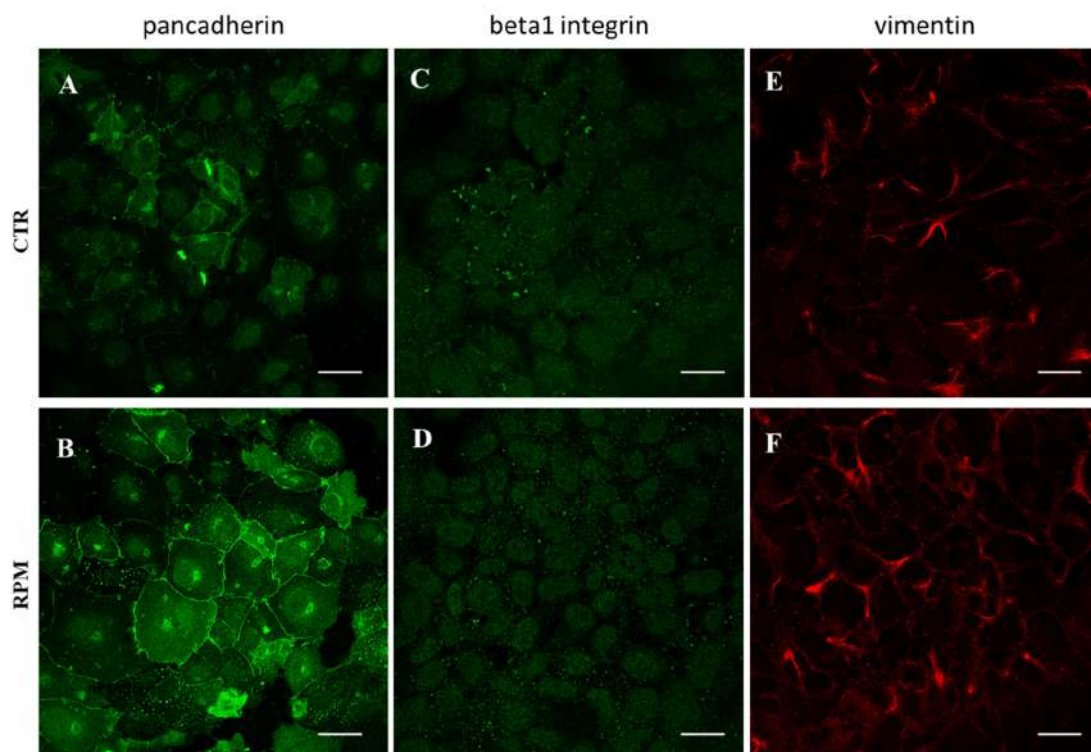


Figure 3. Confocal microscopy analysis of the distribution pattern of pan-cadherin (A,B), beta1 integrin (C,D), and vimentin (E,F) in TCam-2 seminoma cells cultured for 24 h at 1 g (CTR: A,C,E) and in simulated microgravity (RPM: B,D,F). BAR: 60 μ m.

Conversely, the analysis of beta1 integrin localization, did not reveal appreciable changes in the distribution pattern of this protein in RPM cultured samples, indicating that the linkage of the TCam-2 cells to their substrate is not apparently perturbed by simulated microgravity (Figure 3C,D). Notably, as well as for beta1 integrin, also the vimentin-composed intermediate filaments network did not change significantly in 24 h-cultured cells in RPM (Figure 3E,F). The co-localization analyses of beta1 integrin and vimentin in RPM exposed cells revealed that these two proteins did not have overlapping signals. Therefore, it is possible to speculate that they are not implicated in the cell to substrate junctional complex (Figure 5). It is fair to mention that, in a previous work [25], we already investigated the cytoskeletal asset in TCam-2 seminoma cells exposed to simulated microgravity showing that this

condition did not dramatically modify the F-Actin distribution, whereas the microtubule network was significantly perturbed by the RPM condition.

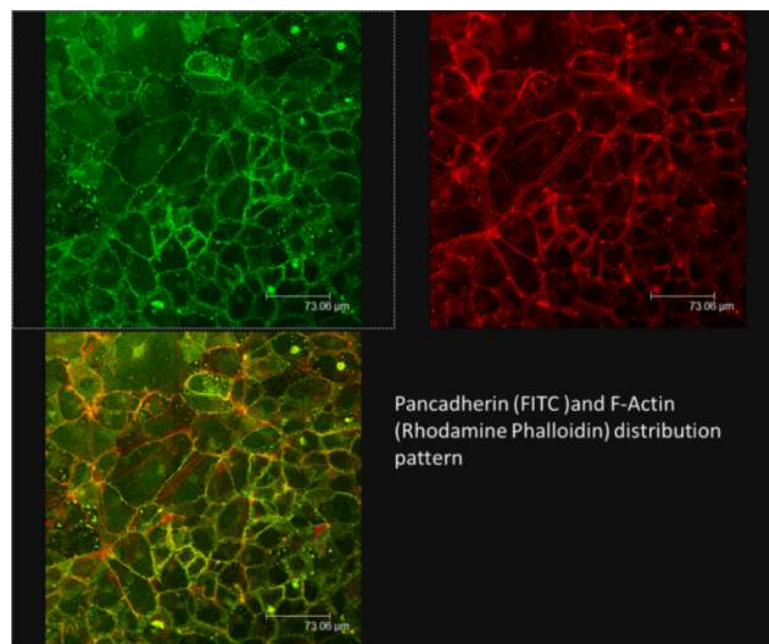


Figure 4. Confocal microscopy analysis of double-fluorescence staining of cadherins (green signal) and F-Actin (red signal) in TCam-2 seminoma cells exposed to simulated microgravity for 24 h. In the bottom panel, the merging picture is reported showing that F-Actin and cadherin signals largely overlap (yellow signal).

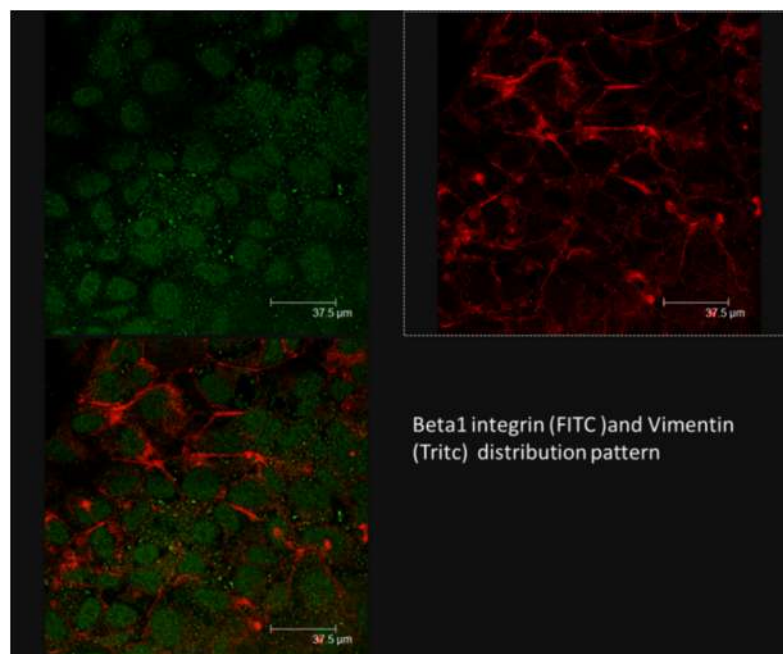


Figure 5. Confocal microscopy analysis of double-immunofluorescence staining of beta1 integrin (green signal) and vimentin (red signal) in TCam-2 seminoma cells exposed to simulated microgravity for 24 h. In the bottom panel, the merging picture is reported showing that Vimentin does not co-localize with beta1 integrin (yellow signal).

A careful analysis of pan-cadherin immunofluorescence experiments let us observe that, in addition to the staining nearby the plasma membrane, a cytoplasmic staining localized at the perinuclear level, compatible with the Golgi network, appeared more evident in RPM exposed samples (Figure 3B). This observation let us hypothesize that, possibly, simulated microgravity exposure not only stimulated the integration of cadherin in the plasma membrane, probably acting directly on cytoplasmic membrane trafficking, but also stimulated its de novo biosynthesis. To verify the expression levels of these adhesion molecules, Western blot analyses were performed. These analyses revealed that cell culturing in RPM conditions promoted a significant increase of cadherin expression levels, while beta1 integrin and vimentin expression levels were not significantly modified with respect to cells cultured at 1 g conditions (Figure 6).

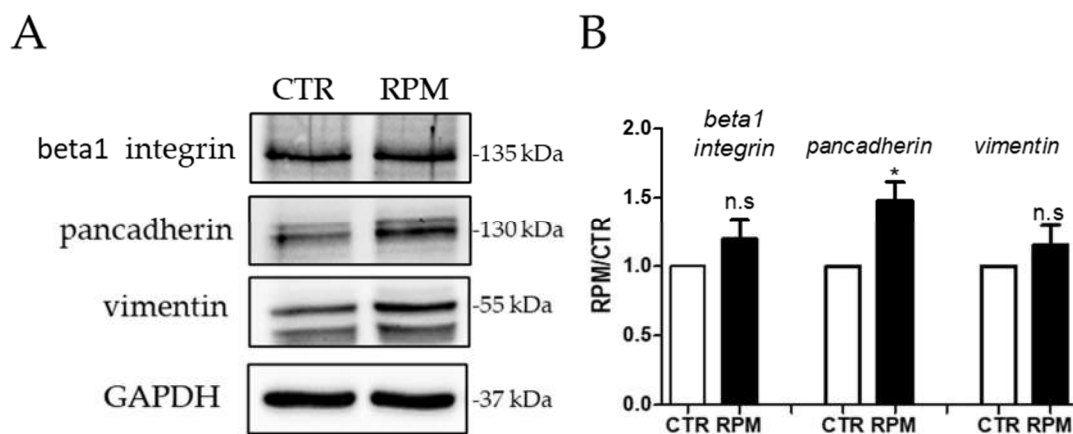


Figure 6. Representative immunoblots of beta1 integrin, pan-cadherin, and vimentin expression levels (A) and the corresponding densitometric analyses (B). These last ones were performed on bands at the corresponding molecular weight of beta1 integrin, pan-cadherin, vimentin, and GAPDH. In addition, they were plotted as a ratio between RPM and CTR, each calculated by the ratio between $OD \times mm^2$ of each band and $OD \times mm^2$ of the respective band in the immunoblot of the GAPDH, considered as a loading control. In the densitometric analyses, data are means \pm SEM from three independent experiments. * $p < 0.05$.

3.4. Antioxidant Compounds Counteract the RPM-Induced Junctional Contacts

The effect of microgravity on cell metabolism and ROS production has been largely explored [32–34]. In a previous paper, we also demonstrated that in TCam-2 cells, simulated microgravity promoted significant, even if transient, increases of intracellular Ca^{2+} , ROS, and $O^{2\bullet-}$ levels, together with higher levels of glucose and lactate in the media, in comparison to 1 g-cultured cells [26]. Notably, in the same paper, we reported that the antioxidant administration (NAC or Trolox) counteracted the already mentioned RPM-induced cell cytoskeletal alterations (such as microtubule disorientation), as well as biological activities such as autophagy induction. In light of these previous results, we tested if RPM-induced effects on the junctional protein, reported above, were ROS-sensible. To this aim, TCam-2 cells were cultured for 24 h at 1 g or in RPM conditions in the absence or presence of Trolox or NAC in the media. Immunofluorescence experiments to test pan-cadherin localization revealed that the presence of DMSO (the solvent of Trolox) alone did not significantly modify the distribution pattern of cadherin observed at 1 g and after 24 h of RPM exposure in basal media. The presence of antioxidants counteracted RPM-induced cadherin localization and upregulation, and Trolox appeared more efficacious than NAC (Figure 7).

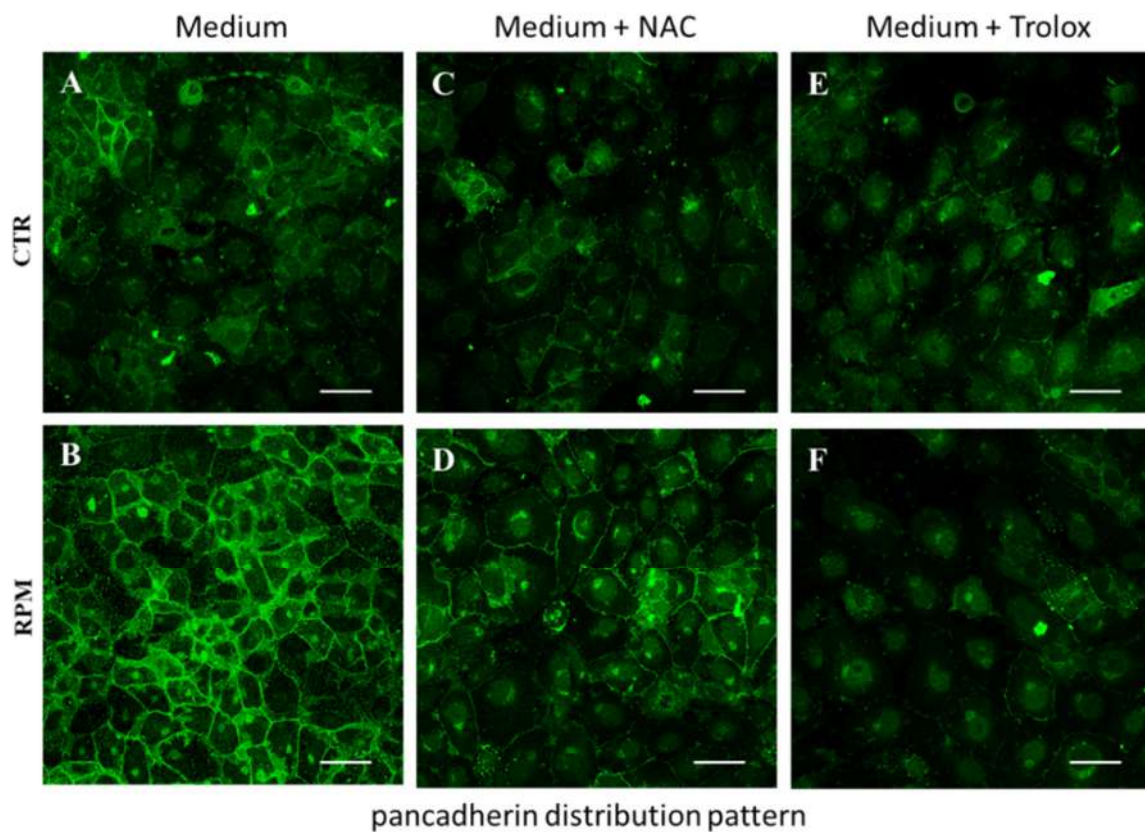


Figure 7. Confocal microscopy analysis of anti-pan-cadherin immunofluorescence. The cells were cultured for 24 h at 1 g (CTR: A,C,E) or in RPM (RPM: B,D,F) in media containing DMSO (Medium + DMSO: A,B), NAC (Medium + NAC: C,D), or Trolox (Medium + Trolox: E,F). BAR: 60 μ m.

It is well known that cadherins interact with beta-catenin and the complex cadherin/catenin is at the basis of the integrity of anchoring junctions that organize and tether microfilaments to maintain cell adhesive properties. This complex integrates intra- and inter-cellular signaling, including the regulation of nuclear functions and transcription pathways [35].

To investigate the molecular feature of the adherent junctions formed under RPM conditions, we evaluated by confocal microscopy the beta-catenin distribution pattern in TCam-2 seminoma cells cultured for 24 h at 1 g and under RPM conditions, in a basal medium or in a medium containing antioxidants (NAC or Trolox). Interestingly, the beta-catenin distribution pattern mimicked the same changes that have been observed analyzing the cadherin distribution (Figure 8). This result indicates that RPM influences not only the cadherin distribution, but even all the complex molecular machinery that guarantee epithelia junctional integrity.

In line with the immunofluorescence results, Western blot analyses revealed that the administration of antioxidants prevents the RPM-induced cadherin upregulation (Figure 9).

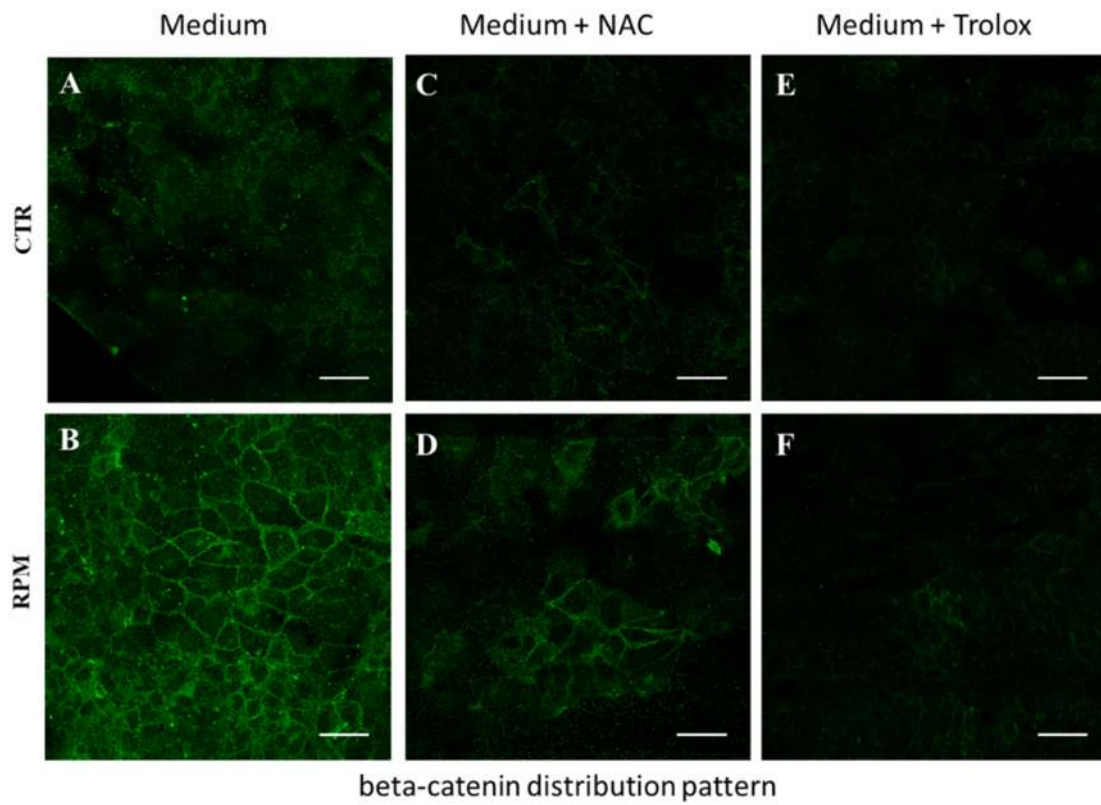


Figure 8. Confocal microscopy analysis of beta-catenin immunofluorescence. The cells were cultured for 24 h at 1 g (CTR: A,C,E) or in RPM (RPM: B,D,F) in media containing DMSO (Medium + DMSO: A,B), NAC (Medium + NAC: C,D), or Trolox (Medium + Trolox: E,F). BAR: 60 μ m.

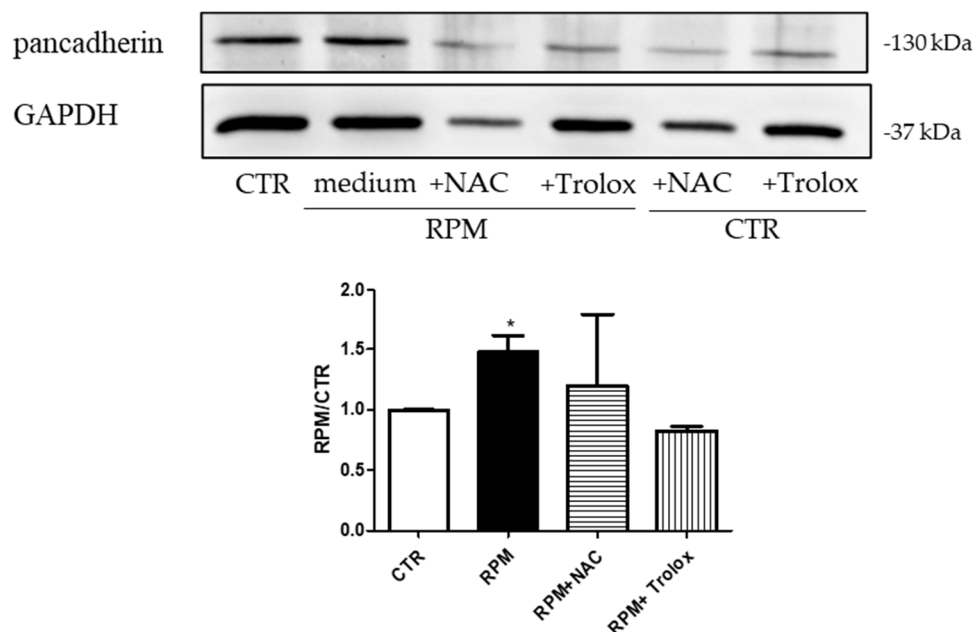


Figure 9. Representative immunoblot of pan-cadherin expression levels, and the corresponding densitometric analysis, plotted as a ratio between RPM and CTR, each calculated by the ratio between $OD \times mm^2$ of each band and $OD \times mm^2$ of the respective band in the immunoblot of the GAPDH, considered as a loading control. In the densitometric analyses, data are means \pm SEM from three independent experiments. * $p < 0.05$.

4. Discussion

The effects of microgravity on cell cytoskeletal and junctional features of mammalian cells *in vitro* has been extensively investigated [15,18,36–38], even if studies on germ cells are still limited [39]. TCam-2 seminoma cells represent a good model to study mitotically active male germ cells, since this transformed cell line partially maintains the germ cell features [24]. We previously demonstrated that simulated microgravity exposure transiently modulated TCam-2 cell microtubule organization, activated autophagy [25], altered mitochondria morphology, and promoted ROS production [26]. Herein, extending our previous studies, we found, in the same cell line, that simulated microgravity upregulates cadherin expression and stimulates its distribution at the membrane level. In line with these results, ultrastructural organized adhesive junctional contacts have been observed together with a jagged interconnected cell-to-cell interface. It is worth mentioning that, even though TCam-2 seminoma cells grow in the culture as an epithelial-like sheet, these cells are not able to form ultra-structurally defined adherent junctions when cultured in basal conditions [24,29]. Notably, this cellular behavior is common in epithelial transformed cells. It is well known that during tumor progression, the loss of cadherins at cell-to-cell junctional contacts, in transformed cells of epithelial origin, drives the worsening of the cellular malignancy, promoting cell instability and metastasis [40,41]. Intercellular contacts mediated by cadherins, are essential even for normal germ cell migration, during embryogenesis, as well as for their maturation. These molecules are in fact finely modulated during germ cell differentiation, being barely detectable in immature cells and finely regulated during spermatogenetic processes. Primordial germ cells (PGC), which are the immature fetal form of male germ cells, express E-cadherin even if at a low level, but seminomas, that represent their malignant counterpart, lose the expression of E-cadherin at cell-to-cell contacts. Moreover, it is worth highlighting that the co-expression of cadherins and beta-catenin correlates with a male germ cell differentiated phenotype [42]. In a previous paper, we obtained the E-cadherin/beta-catenin upregulation in TCam-2 seminoma cells using an egg white complex [29], concluding that “embryonal cues” are probably used by TCam-2 cells to reprogram their proper differentiation attitude despite their malignant transformation. In this paper, we reported a similar cadherin/catenin upregulation and distribution as a consequence of the exposure to simulated microgravity, indicating how the modulation of not only chemical but also physical microenvironmental cues can modify a cell adhesive, and possibly cell differentiating attitude.

It is worth highlighting that many papers reported a negative effect of microgravity on the cadherin expression level and its depletion at the membrane level, in some cellular models such as in MCF-7 cells and human keratinocytes [36,38]. However, recent papers reported an increase of E-cadherin in microgravity exposed fibroblasts, and a pro-angiogenic activity (which means mesenchyme-epithelial transition) of microgravity exposure on human adipose-derived stem cells [43,44]. In light of these published results, we can hypothesize that the effect of real or simulated microgravity exposure on cell adhesion is not univocal, but it depends on the cell differentiation state. This means that the decrease of gravitational force seems to have opposite effects on cells that have epithelial features with respect to those that have connective features or that are derived from mesenchymal progenitors. In this scenario, it is important to be reminded that, even if TCam-2 seminoma cells are of an epithelial origin, they have lost partially their differentiated state, presenting an impaired cell-to-cell adhesion capability. This partial transition to the mesenchymal phenotype, could help understand why the effect of microgravity on TCam-2 seminoma cells is more similar to what was observed in cells of a mesenchymal origin.

In this paper, we also investigated the possible mechanisms in which microgravity can modulate the adhesive attitude of TCam-2 seminoma cells. Notably, we already demonstrated that simulated microgravity induced a transient increase of ROS production [26], and that the antioxidant administration prevented the simulated microgravity-induced autophagy and microtubule disorientation. These results indicated that simulated microgravity-activated ROS are responsible, at least in part, for the microgravity-induced modifications of cell physiology. Notably, autophagy is a way, in which cells react to the changing microenvironment, trying to

rescue their homeostatic phenotype, and it is relevant that this rescue mechanism is activated by microgravity-induced ROS production. In addition, we also reported that, among ROS, there was a significant microgravity-induced increase of the superoxide anion, the main oxidant produced by mitochondria. This together with the observed metabolic alterations and mitochondrial morphology modifications [26] brought us to hypothesize that the mitochondria network, and thus mitochondrial metabolic responses, could be the intracellular targets of the altered extracellular forces. However, there are also other intracellular sources that produce ROS, as the NADPH-oxidase enzymes [45], whose activity cannot be excluded. Noteworthy, it is fair to highlight that, in the last decade, scientific literature has changed the landscape on the actual role of ROS in normal cell physiology. Even though the ROS increase is frequently related to the cell oxidative stress, and in turn to cell damage. Several authors demonstrated that these products of mitochondria metabolism are key elements for cell responses to microenvironmental cues. The double-faced effects of ROS have been highlighted even in cancer progression and therapy [46,47]. This observation leads to a completely novel view of mitochondria functions, the mitohormetic theory, which states that mitochondria are not only energetic organelles but also cell “sensors” which modulate cellular responses [48–52]. This Copernican revolution revealed that many physiological processes are ROS-dependent, and the change of metabolism is not only related to energy production. By this point of view, mild stressors (such as microgravity exposure), triggering ROS production, help cells overcome microenvironmental changes, promoting all the cellular activities necessary to rescue their homeostatic phenotype. To this regard, it has been reported by several authors in different cellular models, that ROS are involved in cell adhesion and cell migration [30,53]. In the present paper, we demonstrated that ROS are necessary for the modification of the cadherin/catenin distribution pattern induced by the microgravity exposure, indicating that the adhesive attitude can be modified by mechanical force modification through modulating metabolism. This stimulates the intriguing hypothesis, which deserves further investigations, that the loss of cadherins in malignant transformation is not a final decision of the cells but could be modulated by controlling metabolic processes.

Author Contributions: Conceptualization, G.R. and M.A.M.; methodology, G.R., C.M., A.C., M.C., K.C.S.; validation, G.R., C.M., A.C., F.F. and M.A.M.; formal analysis, A.C. and C.M.; investigation, A.C., C.M., G.R. and M.A.M.; resources, G.R., M.A.M. and C.S.; data curation, C.S.; writing—original draft preparation, G.R.; writing—review and editing, G.R. and M.A.M.; visualization, G.R., C.M., A.C., M.C., K.C.S., F.F., C.S. and M.A.M.; supervision, G.R. and M.A.M.; project administration, G.R. and M.A.M.; funding acquisition, G.R. and M.A.M. All authors have read and agreed to the published version of the manuscript.

Funding: This work was supported by the Department of Experimental Medicine Università degli Studi della Campania “Luigi Vanvitelli” grant for research to Giulia Ricci (2015 and 2016); FFBAR 2017 to Giulia Ricci; and ASI contract to Giulia Ricci “Shape 2014-018-R.0” CUP F84G14000150005. ASI contract to Maria A. Mariggiò “Shape 2014-018-R.0” CUP F84G14000150005.

Acknowledgments: SEM and TEM analyses were performed at the Electron Microscopy facility of the Department of Experimental Medicine—Università degli Studi della Campania “Luigi Vanvitelli”.

Conflicts of Interest: The authors declare no conflict of interest.

References

1. Locatelli, L.; Cazzaniga, A.; De Palma, C.; Castiglioni, S.; Maier, J.A.M. Mitophagy contributes to endothelial adaptation to simulated microgravity. *FASEB J.* **2020**, *34*, 1833–1845. [[CrossRef](#)] [[PubMed](#)]
2. Liu, C.; Zhong, G.; Zhou, Y.; Yang, Y.; Tan, Y.; Li, Y.; Gao, X.; Sun, W.; Li, J.; Jin, X.; et al. Alteration of calcium signalling in cardiomyocyte induced by simulated microgravity and hypergravity. *Cell Prolif.* **2020**, *53*, e12783. [[CrossRef](#)] [[PubMed](#)]
3. Li, H.; Zhu, H.; Zhang, F.; Dong, X.; Hao, T.; Jiang, X.; Zheng, W.; Zhang, T.; Chen, X.; Wang, P.; et al. Spaceflight Promoted Myocardial Differentiation of Induced Pluripotent Stem Cells: Results from Tianzhou-1 Space Mission. *Stem Cells Dev.* **2019**, *28*, 357–360. [[CrossRef](#)] [[PubMed](#)]

4. Wnorowski, A.; Sharma, A.; Chen, H.; Wu, H.; Shao, N.Y.; Sayed, N.; Liu, C.; Countryman, S.; Stodieck, L.S.; Rubins, K.H.; et al. Effects of Spaceflight on Human Induced Pluripotent Stem Cell-Derived Cardiomyocyte Structure and Function. *Stem Cell Rep.* **2019**, *13*, 960–969. [[CrossRef](#)]
5. Bradbury, P.; Wu, H.; Choi, J.U.; Rowan, A.E.; Zhang, H.; Poole, K.; Lauko, J.; Chou, J. Modeling the Impact of Microgravity at the Cellular Level: Implications for Human Disease. *Front. Cell Dev. Biol.* **2020**, *8*, 96. [[CrossRef](#)]
6. Morabito, C.; Guarnieri, S.; Cucina, A.; Bizzarri, M.; Mariggio, M.A. Antioxidant Strategy to Prevent Simulated Microgravity-Induced Effects on Bone Osteoblasts. *Int. J. Mol. Sci.* **2020**, *21*, 3638. [[CrossRef](#)]
7. Nassef, M.Z.; Kopp, S.; Wehland, M.; Melnik, D.; Sahana, J.; Kruger, M.; Corydon, T.J.; Oltmann, H.; Schmitz, B.; Schutte, A.; et al. Real Microgravity Influences the Cytoskeleton and Focal Adhesions in Human Breast Cancer Cells. *Int. J. Mol. Sci.* **2019**, *20*, 3156. [[CrossRef](#)]
8. Nassef, M.Z.; Kopp, S.; Melnik, D.; Corydon, T.J.; Sahana, J.; Kruger, M.; Wehland, M.; Bauer, T.J.; Liemersdorf, C.; Hemmersbach, R.; et al. Short-Term Microgravity Influences Cell Adhesion in Human Breast Cancer Cells. *Int. J. Mol. Sci.* **2019**, *20*, 5730. [[CrossRef](#)]
9. Bizzarri, M.; Monici, M.; van Loon, J.J. How microgravity affects the biology of living systems. *BioMed Res. Int.* **2015**, *2015*, 863075. [[CrossRef](#)]
10. Ma, Q.; Ma, Z.; Liang, M.; Luo, F.; Xu, J.; Dou, C.; Dong, S. The role of physical forces in osteoclastogenesis. *J. Cell Physiol.* **2019**, *234*, 12498–12507. [[CrossRef](#)]
11. Po, A.; Giuliani, A.; Masiello, M.G.; Cucina, A.; Catizone, A.; Ricci, G.; Chiacchiarini, M.; Tafani, M.; Ferretti, E.; Bizzarri, M. Phenotypic transitions enacted by simulated microgravity do not alter coherence in gene transcription profile. *NPJ Microgravity* **2019**, *5*, 27. [[CrossRef](#)] [[PubMed](#)]
12. Morabito, C.; Lanuti, P.; Caprara, G.A.; Marchisio, M.; Bizzarri, M.; Guarnieri, S.; Mariggio, M.A. Physiological Responses of Jurkat Lymphocytes to Simulated Microgravity Conditions. *Int. J. Mol. Sci.* **2019**, *20*, 1892. [[CrossRef](#)]
13. Nassef, M.Z.; Melnik, D.; Kopp, S.; Sahana, J.; Infanger, M.; Lutzenberg, R.; Relja, B.; Wehland, M.; Grimm, D.; Kruger, M. Breast Cancer Cells in Microgravity: New Aspects for Cancer Research. *Int. J. Mol. Sci.* **2020**, *21*, 7345. [[CrossRef](#)]
14. Masiello, M.G.; Verna, R.; Cucina, A.; Bizzarri, M. Physical constraints in cell fate specification. A case in point: Microgravity and phenotypes differentiation. *Prog. Biophys. Mol. Biol.* **2018**, *134*, 55–67. [[CrossRef](#)]
15. Di Agostino, S.; Botti, F.; Di Carlo, A.; Sette, C.; Geremia, R. Meiotic progression of isolated mouse spermatocytes under simulated microgravity. *Reproduction* **2004**, *128*, 25–32. [[CrossRef](#)]
16. Ricci, G.; Catizone, A.; Esposito, R.; Galdieri, M. Microgravity effect on testicular functions. *J. Gravit. Physiol.* **2004**, *11*, P61–P62.
17. Ricci, G.; Esposito, R.; Catizone, A.; Galdieri, M. Direct effects of microgravity on testicular function: Analysis of histological, molecular and physiologic parameters. *J. Endocrinol. Investig.* **2008**, *31*, 229–237. [[CrossRef](#)]
18. Pellegrini, M.; Di Siena, S.; Claps, G.; Di Cesare, S.; Dolci, S.; Rossi, P.; Geremia, R.; Grimaldi, P. Microgravity promotes differentiation and meiotic entry of postnatal mouse male germ cells. *PLoS ONE* **2010**, *5*, e9064. [[CrossRef](#)]
19. Li, H.Y.; Zhang, H.; Miao, G.Y.; Xie, Y.; Sun, C.; Di, C.X.; Liu, Y.; Liu, Y.Y.; Zhang, X.; Ma, X.F.; et al. Simulated microgravity conditions and carbon ion irradiation induce spermatogenic cell apoptosis and sperm DNA damage. *Biomed. Environ. Sci.* **2013**, *26*, 726–734. [[CrossRef](#)]
20. Strollo, F.; Masini, M.A.; Pastorino, M.; Ricci, F.; Vadrucci, S.; Cogoli-Greuter, M.; Uva, B.M. Microgravity-induced alterations in cultured testicular cells. *J. Gravit. Physiol.* **2004**, *11*, P187–P188.
21. Nowacki, D.; Klinger, F.G.; Mazur, G.; De Felici, M. Effect of Culture in Simulated Microgravity on the Development of Mouse Embryonic Testes. *Adv. Clin. Exp. Med.* **2015**, *24*, 769–774. [[CrossRef](#)]
22. de Jong, J.; Stoop, H.; Gillis, A.J.; Hersmus, R.; van Gurp, R.J.; van de Geijn, G.J.; van Drunen, E.; Beverloo, H.B.; Schneider, D.T.; Sherlock, J.K.; et al. Further characterization of the first seminoma cell line TCam-2. *Genes Chromosomes Cancer* **2008**, *47*, 185–196. [[CrossRef](#)]
23. Eckert, D.; Nettersheim, D.; Heukamp, L.C.; Kitazawa, S.; Biermann, K.; Schorle, H. TCam-2 but not JKT-1 cells resemble seminoma in cell culture. *Cell Tissue Res.* **2008**, *331*, 529–538. [[CrossRef](#)] [[PubMed](#)]
24. Mizuno, Y.; Gotoh, A.; Kamidono, S.; Kitazawa, S. [Establishment and characterization of a new human testicular germ cell tumor cell line (TCam-2)]. *Nihon Hinyokika Gakkai Zasshi* **1993**, *84*, 1211–1218. [[CrossRef](#)] [[PubMed](#)]

25. Ferranti, F.; Caruso, M.; Cammarota, M.; Masiello, M.G.; Corano Scheri, K.; Fabrizi, C.; Fumagalli, L.; Schiraldi, C.; Cucina, A.; Catizone, A.; et al. Cytoskeleton modifications and autophagy induction in TCam-2 seminoma cells exposed to simulated microgravity. *BioMed Res. Int.* **2014**, *2014*, 904396. [[CrossRef](#)] [[PubMed](#)]
26. Morabito, C.; Guarnieri, S.; Catizone, A.; Schiraldi, C.; Ricci, G.; Mariggio, M.A. Transient increases in intracellular calcium and reactive oxygen species levels in TCam-2 cells exposed to microgravity. *Sci. Rep.* **2017**, *7*, 15648. [[CrossRef](#)] [[PubMed](#)]
27. van Roy, F. Beyond E-cadherin: Roles of other cadherin superfamily members in cancer. *Nat. Rev. Cancer* **2014**, *14*, 121–134. [[CrossRef](#)]
28. Casal, J.I.; Bartolome, R.A. Beyond N-Cadherin, Relevance of Cadherins 5, 6 and 17 in Cancer Progression and Metastasis. *Int. J. Mol. Sci.* **2019**, *20*, 3373. [[CrossRef](#)]
29. Ferranti, F.; D'Anselmi, F.; Caruso, M.; Lei, V.; Dinicola, S.; Pasqualato, A.; Cucina, A.; Palombo, A.; Ricci, G.; Catizone, A.; et al. TCam-2 seminoma cells exposed to egg-derived microenvironment modify their shape, adhesive pattern and migratory behaviour: A molecular and morphometric analysis. *PLoS ONE* **2013**, *8*, e76192. [[CrossRef](#)]
30. Lim, S.O.; Gu, J.M.; Kim, M.S.; Kim, H.S.; Park, Y.N.; Park, C.K.; Cho, J.W.; Park, Y.M.; Jung, G. Epigenetic changes induced by reactive oxygen species in hepatocellular carcinoma: Methylation of the E-cadherin promoter. *Gastroenterology* **2008**, *135*, 2128–2140, 2140.e1–2140.e8. [[CrossRef](#)]
31. Yeung, K.T.; Yang, J. Epithelial-mesenchymal transition in tumor metastasis. *Mol. Oncol.* **2017**, *11*, 28–39. [[CrossRef](#)] [[PubMed](#)]
32. Jeong, A.J.; Kim, Y.J.; Lim, M.H.; Lee, H.; Noh, K.; Kim, B.H.; Chung, J.W.; Cho, C.H.; Kim, S.; Ye, S.K. Microgravity induces autophagy via mitochondrial dysfunction in human Hodgkin's lymphoma cells. *Sci. Rep.* **2018**, *8*, 14646. [[CrossRef](#)] [[PubMed](#)]
33. Mori, K.; Uchida, T.; Yoshie, T.; Mizote, Y.; Ishikawa, F.; Katsuyama, M.; Shibamura, M. A mitochondrial ROS pathway controls matrix metalloproteinase 9 levels and invasive properties in RAS-activated cancer cells. *FEBS J.* **2019**, *286*, 459–478. [[CrossRef](#)] [[PubMed](#)]
34. Ran, F.; An, L.; Fan, Y.; Hang, H.; Wang, S. Simulated microgravity potentiates generation of reactive oxygen species in cells. *Biophys. Rep.* **2016**, *2*, 100–105. [[CrossRef](#)] [[PubMed](#)]
35. Tian, X.; Liu, Z.; Niu, B.; Zhang, J.; Tan, T.K.; Lee, S.R.; Zhao, Y.; Harris, D.C.; Zheng, G. E-cadherin/beta-catenin complex and the epithelial barrier. *J. Biomed. Biotechnol.* **2011**, *2011*, 567305. [[CrossRef](#)] [[PubMed](#)]
36. Lin, X.; Zhang, K.; Wei, D.; Tian, Y.; Gao, Y.; Chen, Z.; Qian, A. The Impact of Spaceflight and Simulated Microgravity on Cell Adhesion. *Int. J. Mol. Sci.* **2020**, *21*, 3031. [[CrossRef](#)]
37. Zhang, X.; Li, L.; Bai, Y.; Shi, R.; Wei, H.; Zhang, S. Mouse undifferentiated spermatogonial stem cells cultured as aggregates under simulated microgravity. *Andrologia* **2014**, *46*, 1013–1021. [[CrossRef](#)]
38. Ranieri, D.; Proietti, S.; Dinicola, S.; Masiello, M.G.; Rosato, B.; Ricci, G.; Cucina, A.; Catizone, A.; Bizzarri, M.; Torrisi, M.R. Simulated microgravity triggers epithelial mesenchymal transition in human keratinocytes. *Sci. Rep.* **2017**, *7*, 538. [[CrossRef](#)]
39. Motabagani, M.A. Morphological and morphometric study on the effect of simulated microgravity on rat testis. *Chin. J. Physiol.* **2007**, *50*, 199–209.
40. Zetter, B.R. Adhesion molecules in tumor metastasis. *Semin Cancer Biol.* **1993**, *4*, 219–229.
41. Cavallaro, U.; Christofori, G. Multitasking in tumor progression: Signaling functions of cell adhesion molecules. *Ann. N. Y. Acad. Sci.* **2004**, *1014*, 58–66. [[CrossRef](#)] [[PubMed](#)]
42. Honecker, F.; Kersemaekers, A.M.; Molier, M.; Van Weeren, P.C.; Stoop, H.; De Krijger, R.R.; Wolffenbuttel, K.P.; Oosterhuis, W.; Bokemeyer, C.; Looijenga, L.H. Involvement of E-cadherin and beta-catenin in germ cell tumours and in normal male fetal germ cell development. *J. Pathol.* **2004**, *204*, 167–174. [[CrossRef](#)] [[PubMed](#)]
43. Buken, C.; Sahana, J.; Corydon, T.J.; Melnik, D.; Bauer, J.; Wehland, M.; Kruger, M.; Balk, S.; Abuagela, N.; Infanger, M.; et al. Morphological and Molecular Changes in Juvenile Normal Human Fibroblasts Exposed to Simulated Microgravity. *Sci. Rep.* **2019**, *9*, 11882. [[CrossRef](#)]
44. Ratushnyy, A.; Ezdakova, M.; Yakubets, D.; Buravkova, L. Angiogenic Activity of Human Adipose-Derived Mesenchymal Stem Cells Under Simulated Microgravity. *Stem Cells Dev.* **2018**, *27*, 831–837. [[CrossRef](#)] [[PubMed](#)]
45. Bedard, K.; Krause, K.H. The NOX family of ROS-generating NADPH oxidases: Physiology and pathophysiology. *Physiol. Rev.* **2007**, *87*, 245–313. [[CrossRef](#)] [[PubMed](#)]

46. Poljsak, B.; Milisav, I. The Role of Antioxidants in Cancer, Friends or Foes? *Curr. Pharm. Des.* **2018**, *24*, 5234–5244. [[CrossRef](#)] [[PubMed](#)]
47. Moldogazieva, N.T.; Lutsenko, S.V.; Terentiev, A.A. Reactive Oxygen and Nitrogen Species-Induced Protein Modifications: Implication in Carcinogenesis and Anticancer Therapy. *Cancer Res.* **2018**, *78*, 6040–6047. [[CrossRef](#)] [[PubMed](#)]
48. Sedlackova, L.; Korolchuk, V.I. The crosstalk of NAD, ROS and autophagy in cellular health and ageing. *Biogerontology* **2020**, *21*, 381–397. [[CrossRef](#)]
49. Yun, J.; Finkel, T. Mitohormesis. *Cell Metab.* **2014**, *19*, 757–766. [[CrossRef](#)]
50. Reczek, C.R.; Chandel, N.S. ROS-dependent signal transduction. *Curr. Opin. Cell Biol.* **2015**, *33*, 8–13. [[CrossRef](#)]
51. Schieber, M.; Chandel, N.S. TOR signaling couples oxygen sensing to lifespan in *C. elegans*. *Cell Rep.* **2014**, *9*, 9–15. [[CrossRef](#)] [[PubMed](#)]
52. Chandel, N.S. Mitochondria as signaling organelles. *BMC Biol.* **2014**, *12*, 34. [[CrossRef](#)]
53. Chiarugi, P. Reactive oxygen species as mediators of cell adhesion. *Ital. J. Biochem.* **2003**, *52*, 28–32. [[PubMed](#)]

Publisher’s Note: MDPI stays neutral with regard to jurisdictional claims in published maps and institutional affiliations.



© 2020 by the authors. Licensee MDPI, Basel, Switzerland. This article is an open access article distributed under the terms and conditions of the Creative Commons Attribution (CC BY) license (<http://creativecommons.org/licenses/by/4.0/>).